

JOURNAL OF THE PHYSICAL SOCIETY OF JAPAN Vol. 13, No. 3, MARCH, 1958

## Optical and Electrical Properties of Tin Oxide Films

By Kozo ISHIGURO, Taizo SASAKI, Toshihiro ARAI  
and Isamu IMAI

*Department of Physics, College of General Education;  
Institute of Science and Technology,  
University of Tokyo*

(Received June 29, 1957)

The electrical and optical properties of the transparent conducting tin oxide films were studied experimentally. The observed Hall effect and Seebeck effect show that the present specimens are *n*-type conductor whose carrier density is  $10^{19} \sim 10^{20} \text{ cm}^{-3}$ . The optical measurements made it clear that the fundamental energy gap was about 4 eV and the plasma frequency of the conducting carriers lied in the near infrared region. By comparing the observed optical transmission and reflection with the theoretical values which can be calculated with the electrically measured constants, the effective mass of the carriers was determined to be about 1/5 of the free electron mass. It will be discussed in conclusion that, to satisfy the thermoelectric power relation with this small effective mass, we must assume that the Coulomb scattering of impurity ions is the predominant scattering mechanism in the transparent conducting tin oxide films.

### §1. Introduction

Since the interesting properties of transparent conducting coating on glass surface were discovered, a large number of experimental works in this field have been reported<sup>1)</sup>. But these have been confined almost exclusively to the refinement of the method of preparation and very few papers have referred to the analysis of their physical properties. The object of the present paper is to report on the experimental results carried out in our laboratory to make clear the optical and electrical properties of the typical transparent conducting coating, tin oxide film. In particular, the contribution of the free carriers,

whose nature can be estimated from the electrical measurements, to the optical properties in the near infrared region will be discussed in some detail.

### §2. Preparation of Samples

Among the various methods of preparation, the simplest one was adopted. Namely, one component solution of  $\text{SnCl}_4 \cdot 5\text{H}_2\text{O}$  crystal or  $\text{SnCl}_4$  liquid in distilled water or in ethyl alcohol was sprayed by a small atomizer on the glass, fused silica or rock salt plates. The effect of mixing the impurities of III or V valency according to Verwey's principle of controlled valency<sup>2)</sup> will not be discussed in

the present paper.

As shown in Fig. 1, the substrate was held downward in a main cylindrical electric furnace and the solution was sprayed onto it from the underlying atomizer. After passing through the preheating furnace, the atomized fog of  $\text{SnCl}_4$  was poured upon the heated substrate. The adequate temperature of the main furnace was  $500\sim 600^\circ\text{C}$ .

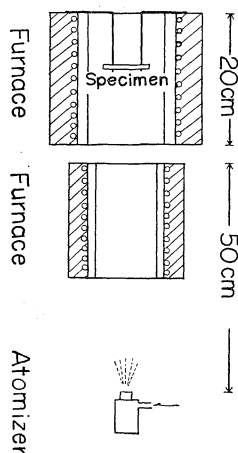


Fig. 1. Arrangement for preparing samples.

According to the electron diffraction observation, the main pattern coincides with that of  $\text{SnO}_2$  and the rings are fairly sharp, indicating that the film is composed of crystallites not so small as to be interpreted as amorphous state.

### § 3. Electrical Properties

The experimental arrangement used for the conductivity measurement is shown schematically in Fig. 2. Knowing the film thickness, the conductivity of the sample can be calculated from the potential difference between the fixed points A and B, if a constant current is maintained in the sample from left to right in the figure. The potential difference was measured by the usual potentiometric method whose sensitivity was ca. 5 micro volts. To assure the ohmic contacts in the arrangement, careful pre-examinations had been repeated until the result was satisfactory. Table I summarizes the measured values for several different samples.

The Seebeck E.M.F.  $\theta$  was also measured by giving a temperature difference of several degrees between the point contacts A and B.

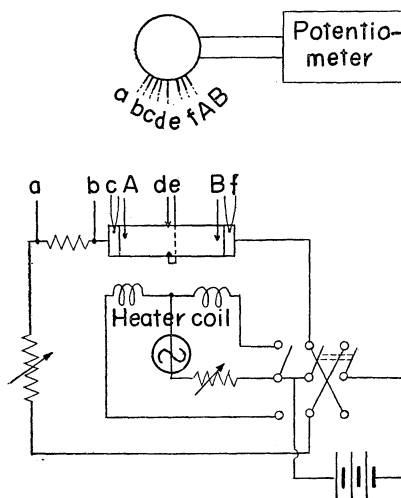


Fig. 2. Schematic diagram of circuit used for measurements of electric properties.

Since the Seebeck E.M.F. of tin oxide is much larger than that of copper which was used as point contact probes, the direction of thermoelectric power directly suggests the type of the free carriers in tin oxide. The conclusion is that our specimens are *n*-type carriers in accordance with Aichison<sup>3)</sup> and Bauer<sup>4)</sup>.

The temperature dependence of  $\theta$  is given by the formula<sup>5)</sup>

$$\left. \begin{aligned} \Theta &= -e \frac{d\theta}{dT} = \left( \frac{p}{6} + \frac{1}{2} \right) \pi^2 k / \xi \\ &\quad \text{(in the degenerate case)} \\ &= \left( \frac{p}{2} + \frac{5}{2} - \xi \right) k \\ &\quad \text{(in the non-degenerate case)} \end{aligned} \right\} \quad (1)$$

where

$$\xi = \zeta / kT,$$

$$\zeta = \text{Fermi energy},$$

$$p = \text{scattering index defined from the proportionality of relaxation time } \tau \text{ to } v^p.$$

$p$  is an adjustable parameter chosen so as to give the best representation of  $\tau$ . The limiting values of  $p$  are  $-1$  and  $3$ . The former corresponds to the scattering by the acoustical lattice vibrations and the latter to the Coulomb scattering by ionized atoms. In our specimens, the number of free electrons is such that they cannot be treated as a non-degenerate gas and it is necessary to consider them a transition case from classical to quantum statistics.

The correct Fermi energy and effective

Table I. Electrical constants of tin oxide films

Sample Number		15	16	18
Film thickness $l$ (m $\mu$ )		110	42	82
Conductivity	$\sigma$ ( $\Omega$ cm) <sup>-1</sup> (room temp.)	430	63	155
	$d\sigma/dT$	$\sim 0$	$> 0$	$> 0$
Hall coeff. $H_R$ (cm <sup>3</sup> /coul) (room temp)		0.075	0.145	0.11
Seebeck E.M.F. ( $\mu$ V/deg)	$\mathcal{E} = \frac{d\Theta}{dT}$ (room temp.)	70	122	95
	$d\mathcal{E}/dT$	0.18	$\sim 0.00$	—
Photo conductivity	rise time (min)	2~3	1~3	1~3
	decay time (min)	$\sim 7$	5~10	3~4
	$\Delta\sigma/\sigma$ (%)	0.3	—	1~2

Sample Number	15			18		
Carrier density $n$ (cm <sup>-3</sup> ) (room temp.)	$8.4 \times 10^{19}$			$5.8 \times 10^{19}$		
Hall mobility $\mu_H$ (cm <sup>2</sup> /volt. sec)(room temp.)	32			17		
Scattering index $p$	-1	0	3	-1	0	3
Fermi level $\zeta = (h^2/8m^*)(3n/\pi)^{2/3}$ (ev)	0.12	0.18	0.36	0.08	0.12	0.23
Effective mass $m^*/m$	0.59	0.39	0.20	0.71	0.47	0.24
Degenerate temp. $T_{deg}$ (K <sup>o</sup> )	1400	2600	4100	900	1400	2700
Relaxation time $\tau$ (sec)	$1.1 \times 10^{-14}$	$7.1 \times 10^{-15}$	$3.6 \times 10^{-15}$	$6.7 \times 10^{-15}$	$4.5 \times 10^{-15}$	$2.2 \times 10^{-15}$
Mean free path $l = (2\zeta/m^*)^{1/2}\tau$	29 Å			13 Å		
Plasma frequency $\nu_p = (\sigma/\pi\tau)^{1/2}$ (sec <sup>-1</sup> )	$1.07 \times 10^{14}$	$1.32 \times 10^{14}$	$1.84 \times 10^{14}$	$0.82 \times 10^{14}$	$1.00 \times 10^{14}$	$1.42 \times 10^{14}$
Relaxation frequency $\nu_A = (1/2\pi\tau)$ (sec <sup>-1</sup> )	$1.48 \times 10^{13}$	$2.24 \times 10^{13}$	$4.37 \times 10^{13}$	$2.38 \times 10^{13}$	$3.54 \times 10^{13}$	$7.25 \times 10^{13}$
$\nu_B$ (sec <sup>-1</sup> )	$1.559 \times 10^{15}$					
$\bar{\nu}_B$ (sec <sup>-1</sup> )	$2.802 \times 10^{15}$					
$(1/l)^3$ (cm <sup>-3</sup> )	$4.1 \times 10^{19}\dagger$			$4.4 \times 10^{20}$		

† It may be interesting to notice that  $n \approx (1/l)^3$  in the present case.

mass of carriers may be estimated from (1) by appropriate interpolations. However, as it is generally admitted that the effective mass  $m^*$  determined from the Seebeck effect gives too small value, we did not adopt the calculated value itself but assumed that the upper and lower limits of the effective mass were the free electron mass  $m$  and 1/10 of it respec-

tively. The optical transmission and reflection calculated assuming these limiting values of the effective mass are compared with the measured values which are to be given in the next section.

The samples of relatively high electric conductivity change their conductivity neither by temperature variation nor by evacuation.

But the low conductivity samples were rather unstable and the results obtained were similar to those of G. Bauer<sup>4)</sup>, who investigated the temperature dependence of conductivity, Seebeck E.M.F. and Hall coefficient of tin oxide films prepared by the oxidation of Sn films evaporated on fused quartz plates. Assuming that the temperature dependence of the low conductivity specimens is given by

$$\sigma = a \exp(-\varepsilon/kT),$$

the activation energy  $\varepsilon$  is estimated at 0.01~0.04 eV. By evacuation, however, the conductivity increases to about 10 times this value under the normal condition. It may be concluded, therefore, that the low conductivity samples are typical reduction type semiconductors, the excess Sn atoms supplying the conduction electrons.

A ceramic specimen with dimension  $10 \times 2 \times 2$  mm showed the resistance of about  $10^{11}$  ohms, which remained unchanged even after the bombardment with 2 MeV deuterons of ca.  $10^{14}$  per  $\text{cm}^2$  density generated by the cyclotron of Inst. of Science and Technology\*. When the same specimen was evacuated, however, the resistance was found to decrease remarkably. This may be due to the escape of oxygen atoms from the surface layer.

The Hall constant  $R_H$  was obtained with some difficulties, since the effect was fairly small, especially for high conductivity samples whose constants were about  $R_H = 0.075 \text{ cm}^3/\text{coul}$ . The measured constants indicate that the specimens are  $n$ -type in accordance with the Seebeck effect measurement. From the Hall constant of the typical sample No. 15, we estimate the carrier concentration  $N$  and Hall mobility  $\mu_H$  as follows:

$$N = 8.4 \times 10^{19} \text{ cm}^{-3}$$

$$\mu_H = 32 \text{ cm}^2/\text{volt} \cdot \text{sec}.$$

#### § 4. Optical Properties

The transmission and reflection in the wavelength region from 0.25 to  $4.0 \mu$  were measured by a small quartz spectro-photometer, and the transmission of the longer wavelength region was recorded by a Parkin Elmer spectro-photometer and a rock salt double

monochrometer, Koken Type 301. As the substrates, fused quartz and rock salt plates were used. Fused quartz is superior than rock salt in the durability for the humidity and the mechanical impinging. Since it does not transparent for longer wavelength region than  $4 \mu$ , however, we must use rock salt plate for the measurements in the region from  $4 \mu$  to  $15 \mu$ . Fig. 3 shows transmissivity

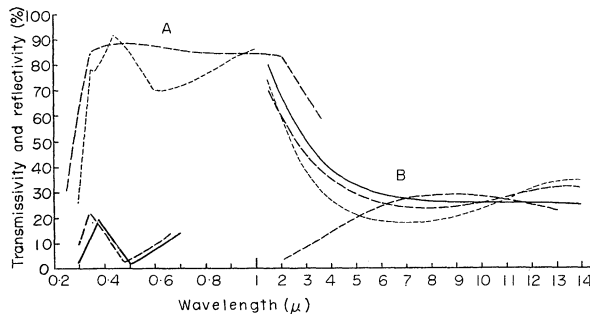


Fig. 3. Observed transmissivity and reflectivity of tin oxide films as a function of wavelength.

A: fused quartz substrate.

B: rock salt substrate.

— } represent different specimens  
 --- }  
 ---- }

versus wavelength curves. The substrate of sample A was a fused quartz plate and that of sample B was a rock salt plate. The specimens sprayed on rock salt plate generally show very low D.C. conductivity. Microscopic observation revealed that many cracks are present on these specimens, however, and the A.C. measurement proved that the conductivity remarkably increased already at 10 k.c. Therefore, these low D.C. conductivity is not the intrinsic nature of the film on rock salt substrate but is caused only by a macroscopic boundary effect of the cracks. Then the apparent low D.C. conductivity will not have any important influence on optical properties, if the scattering loss of the incident light by these cracks is corrected to give a smooth transmission curve connecting the values for the quartz and rock salt substrates.

A general survey of the curves shows that the specimens are almost perfectly transparent in visible region and the fundamental absorption begins at about  $0.3 \mu$  extending to shorter wave length. In the infrared region, the transmissivity decreases gradually whereas

\* The bombardment was carried out by the courtesy of Prof. K. Ôno.

the reflectivity begins to increase\*.

The absorption coefficients at the fundamental absorption edge are shown in Fig. 4. The correlation between the absorption coefficient and the D.C. conductivity was not detected.

The refractive index in the transparent region and the film thickness were obtained from the determination of the wavelengths corresponding to the interference maxima and minima and the reflectivities at these wavelengths. The film thickness was also checked by Tolansky's multiple beam interference method, and the refractive indices measurement was supplemented by Abelès' reflection method<sup>7)</sup>.

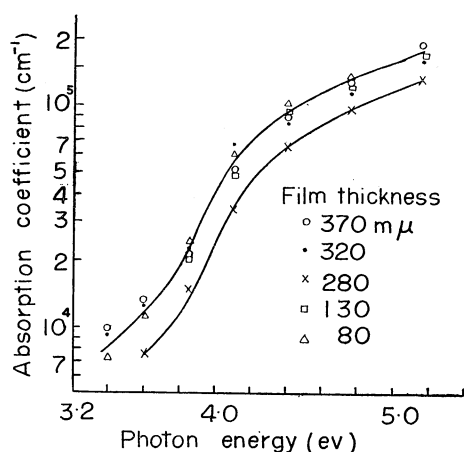


Fig. 4. Absorption coefficient at the fundamental absorption edge as a function of photon energy.

Some measurements were also made of the photo-conductivity. The photo current of about 1% of the dark current was observed when the specimen was exposed to light from a high pressure mercury lamp with a filter transmitting only ultra violet light. This observation confirms that the fundamental absorption edge corresponds to the energy gap between the valence band and the conduction band. But it should be noticed that the rise and decay time of photo-conductivity of

the present specimens are several minutes or more. Since the correction of the thermo-electric effect induced by the temperature rise of the specimen by illumination of intense light has been considered, these slow time response cannot be explained by the thermal effect. It is not clear at present why such slow time response should occur in the specimens with so many dark free carriers which will immediately fill up the holes made by photo electrons.

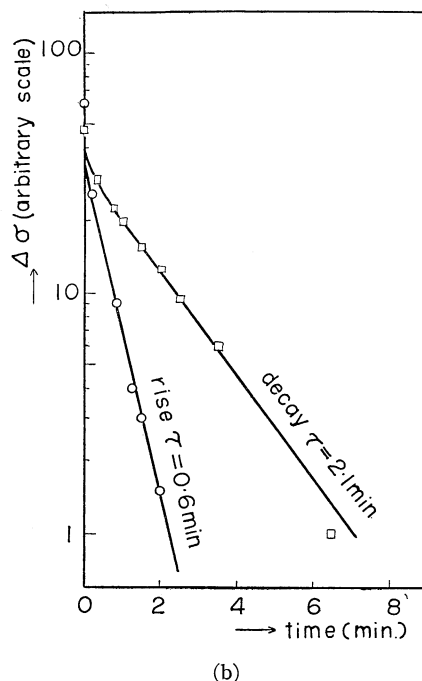
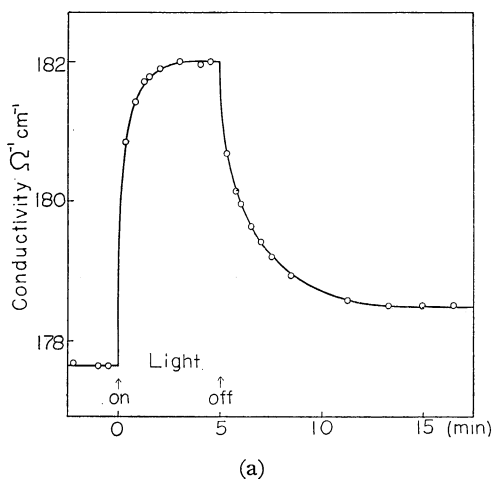


Fig. 5 (a), (b). Time dependency of photo-conduction.

\* Aitchison reported that tin oxide was transparent from 0.2 to 14 microns<sup>3)</sup>. But our observations do not support his results. He adopted reflection method and the sensitivity of the reflection method is high only when the absorption is very large and this may explain the cause of his neglect of absorption.

### §5. Unified Discussions of Electrical and Optical Properties<sup>9)</sup>

E. Kanai<sup>8)</sup> proposed to adopt the well known optical theory of metals to explain the characteristics of tin oxide. He attributes the difference between the usual metals and tin oxide to the difference of the free carrier concentration. Though the plasma frequency of metals of high carrier concentration lies in the ultra violet region, that of tin oxide lies in the near infrared owing to the low carrier concentration. In his opinion, this is the cause of the optical transparency of tin oxide in spite of its metallic conduction. If this is the case, the measurements of optical properties may afford a supplemental method to determine effective mass and the scattering mechanism of free carriers even when the specimen is unstable for temperature change. This will be discussed below.

In germanium, the plasma frequency lies in the far infrared region owing to the low concentration of carriers, which makes its study very difficult. But in the case of semi metallic conductor such as tin oxide, we can investigate the optical anomalies expected at the plasma frequency without large experimental difficulty.

Let us suppose that the refractivity of tin oxide is caused by the combined effect of the intrinsic absorption continuum lying in the ultra violet region corresponding to the excitation of oxygen ions and the infrared absorption by the ohmic conduction of free carriers

and, therefore, that it is not necessary to consider the absorption by lattice vibration.

The dispersion of refractive index, then, is given by the usual Drude-Krönig-Fujioka's formula

$$n^2 - k^2 = A_\nu - \frac{\nu_P^2}{\nu^2 + \nu_A^2}$$

$$2nk = \frac{\nu_P^2 \nu_A}{\nu^2 + \nu_A^2} \frac{1}{\nu} + B_\nu \nu,$$

where

$n - ik$  = complex refractive index,

$\nu_P$  = plasma frequency

$$= (e^2 N / m^* \pi)^{1/2}$$

$$= (\sigma / \pi \tau)^{1/2},$$

$$\nu_A = 1 / 2\pi\tau,$$

$$A_\nu = \bar{\nu}_B^2 / (\nu_B^2 - \nu^2),$$

$$B_\nu = \bar{\nu}_B \nu_C / (\nu_B^2 - \nu^2)^2$$

and  $\nu_B$ ,  $\bar{\nu}_B$ ,  $\nu_C$  represent the mean effect of the fundamental electronic transitions in the ultra violet region.

For the longer wavelength region than the visible, one may put  $B_\nu = 0$ , since the experiment shows that no absorption is present in the visible region.  $\nu_B$  and  $\bar{\nu}_B$  can be calculated from the observed refractive indices in the visible region, and  $\nu_P$  and  $\nu_A$  are determined from the electrical measurements. With these values, one can calculate the complex refractive index at any given frequency in the infrared region as shown in Table II.

If we assume that the film thickness is so large, say 10  $\mu$ , that the interference effect

Table II. Calculated refractive index and extinction coefficient as a function of wavelength

$\lambda(\mu)$	$m^* = m$		$m^* = 0.35m$		$m^* = 0.1m$		experiment	
	$n$	$k$	$n$	$k$	$n$	$k$	$n$	$k$
0.5	1.943	0.000	1.934	0.000	1.900	0.000	1.96	0.00
0.7	1.860	0.000	1.843	0.000	1.774	0.020	1.85	0.00
0.9	1.822	0.000	1.792	0.000	1.675	0.046		
1.0	1.811	0.000	1.774	0.000	1.633	0.062		
2.0	1.708	0.000	1.565	0.042	1.156	0.567		
3.0	1.604	0.022	1.227	0.177	1.187	1.414		
4.0	1.433	0.050	0.786	0.627	1.479	2.012		
5.0	1.186	0.114	0.696	1.311	1.792	2.448		
10.0	0.508	1.991	1.504	3.397	3.072	3.756		
15.0	0.905	3.435	2.471	4.652	3.997	4.599		
20.0	1.421	4.609	3.350	5.544	4.746	5.280		
50.0	4.881	8.986	6.965	8.647	7.840	8.188		

may be neglected, then one can write the reflectivity  $R$  and transmissivity  $T$

$$R = \frac{(n_2 - n)^2 + k^2}{(n_2 + n)^2 + k^2},$$

$$T = \frac{16n_0n_2(n^2 + k^2)}{\{(n + n_2)^2 + k^2\}\{(n + n_0)^2 + k^2\}} e^{-\alpha l},$$

where  $n_0$  is the refractive index of the substrate and  $n_2$  is that of the incident side medium. (Fig. 7)

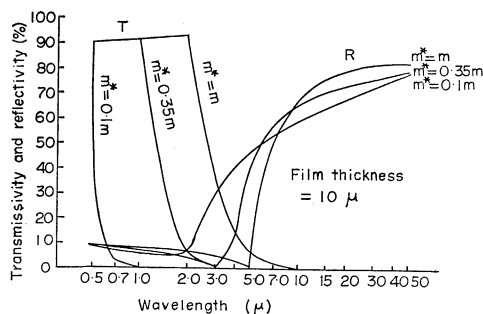


Fig. 6. Transmissivity and reflectivity calculated as a function of wavelength with the assumed effective mass;  $m^*=0.1m$ ,  $0.35m$  and  $m$ . (film thickness= $10\mu$ ).

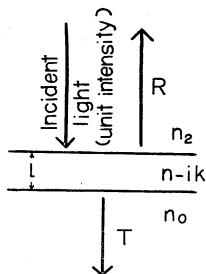


Fig. 7. Schematic explanation of transmissivity and reflectivity of film.

The calculated values are shown in Fig. 6. It is expected from them that the reflection increases remarkably for wavelengths longer than the wavelength corresponding to plasma frequency, and that the transmission decreases rapidly at the same wavelength region<sup>13)</sup>. However, the actual specimens do not have such a large thickness and are only  $0.1\sim 0.3\mu$  thick. Then one cannot neglect the interference effect and must use the exact formula which involves the interference effect<sup>10)</sup>:

$$R = e^{-\alpha l} \left\{ \left( \frac{M_2}{N_2} \right)^2 e^{\alpha l} + \left( \frac{M_0}{N_0} \right)^2 e^{-\alpha l} - 2 \left( \frac{M_0 M_2}{N_0 N_2} \right) \cos(D + \Phi) \right\} |f|^2,$$

$$T = e^{-\alpha l} \frac{16n_0n_2(n^2 + k^2)}{\{(n + n_2)^2 + k^2\}\{(n + n_0)^2 + k^2\}} |f|^2,$$

and

$$|f|^2 =$$

$$= \frac{e^{\alpha l}}{\left\{ e^{\alpha l} + \left( \frac{M_0 M_2}{N_0 N_2} \right)^2 e^{-\alpha l} - 2 \left( \frac{M_0 M_2}{N_0 N_2} \right) \cos(D + \Psi) \right\}},$$

where

$$n_j - n_1 = M_j \exp i\phi_j \quad M_j^2 = (n_j - n)^2 + k^2$$

$$n_j + n_1 = N_j \exp i\theta_j \quad N_j^2 = (n_j + n)^2 + k^2$$

( $j=0$  or  $2$ )

$$(M_0 M_2 N_0 N_2) \cos \Phi$$

$$= (n^2 + k^2)^2 + n_0^2 n_2^2 - (n_0^2 + n_2^2)(n^2 + k^2) + 4n_0 n_2 k^2$$

$$(M_0 M_2 N_0 N_2) \sin \Phi = 2k(n_0 - n_2)(n^2 + k^2 + n_0 n_2)$$

$$(M_0 M_2 N_0 N_2) \cos \Psi$$

$$= (n^2 + k^2)^2 + n_0^2 n_2^2 - (n_0^2 + n_2^2)(n^2 + k^2) - 4n_0 n_2 k^2$$

$$(M_0 M_2 N_0 N_2) \sin \Psi = 2k(n_0 + n_2)(n^2 + k^2 - n_0 n_2).$$

In Fig. 8, the results of the calculations for the effective mass  $m^*=0.1m$ ,  $0.35m$  and  $m$  are

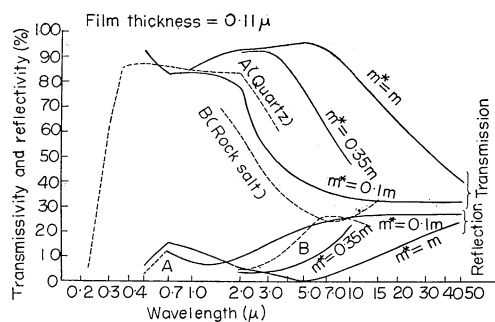


Fig. 8. Comparison of the observed transmissivity and reflectivity of tin oxide film with the calculated values with the assumed effective mass of free carriers:  $m^*=0.1m$ ,  $0.35m$  and  $m$ . Full line=calculation, Dotted line=observation (film thickness= $0.11\mu$ ).

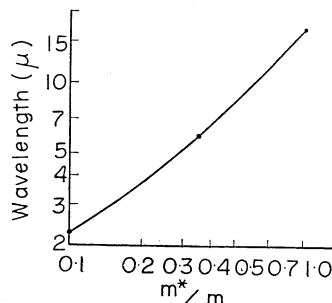


Fig. 9. Calculated wavelength corresponding to transmissivity 70% of tin oxide film of  $0.11\mu$  thick as a function of  $m^*/m$ .

compared with the experimental values (No. 15) where  $m$  is the free electron mass. To make the calculated one coincide with the experimental value, one may be inclined to adopt  $m^* \approx 0.15m$ . (Fig. 9) Then, if the equation (1) is valid for the present case, the scattering index  $p$  must be 3 in order to give such effective mass in the degenerate case (Table I). Then it may be concluded that, in the present specimens, the Coulomb scattering by ionized atoms is the rather predominant scattering mechanism.

## § 6. Discussions

The electrical and optical properties of tin oxide films mentioned above don't have the remarkable differences from the other oxides such as  $\text{In}_2\text{O}_3$ ,  $\text{CdO}$ ,  $\text{ZnO}$  etc., except the fact that the density of the free carriers are easily increased by the simple method and the films are strong and durable. Furthermore, it is reported by several authors<sup>11)</sup> that the transparent electrodes are also made by  $\text{In}_2\text{O}_3$  and  $\text{CdO}$  films prepared by sputtering method in an atmosphere of the adequate oxygen pressure and the mobilities of electrons are also in the range of  $1 \sim 100 \text{ cm}^2/\text{volt} \cdot \text{sec}$ . When these oxides are heated above  $200^\circ\text{C}$ , complex irreversible change due to adsorption, dissociation and diffusion of oxygen occurs and the interpretation of conductivity versus temperature curves must be cautions of these effects and the details of our experimental results of conductivity change with temperature of  $\text{SnO}$  and  $\text{SnO}_2$  films will be reported later in another paper. Considering these circumstances, one of the interesting points of the study of  $\text{SnO}_2$  films is to determine the source of the free carriers of such large density and our conclusion that the impurity scattering of free carriers is the predominant process in the conduction mechanism may be suggestive. But it must be noticed that the conclusion was derived by applying the well known usual theory of metals and only the scattering of lattice vibration of the acoustical mode was considered and the effect of optical vibration was neglected. But if the ionic character of the binding of  $\text{SnO}_2$  crystal is large, such approximation may not be allowed.

Percentage ionic character  $P$  of  $\text{SnO}$  bonding is given by<sup>12)</sup>

$$P = 16|x_{\text{Sn}} - x_0| + 3.5|x_{\text{Sn}} - x_0|^2$$

$$= 37.3\%$$

where  $x_{\text{Sn}} \approx 1.8$  and  $x_0 = 3.5$ . This is fairly small comparing with the values of alkali halides. However, considering the fact that  $\text{SnO}_2$  crystal is rutile type and Madelung constant is very large, the ionic character in bonding might be the considerable amount and the neglect of the interaction of the electron wave with the optical vibration of lattice may not be good approximation. On the other hand, however, the fact that the effective mass of our sample is small and same order with the homopolar crystals such as  $\text{Ge}$  and  $\text{Si}$  support the opposite stand point that the effect of optical mode is small. Because, with the increasing ionic character of the lattice, the free electron will be afforded the nature of polaron and the mass must be increased. The measurements of the absorption of infrared radiation in the residual ray region are desirable to make this problem clear. Finally, it will need some explanation that whereas the carrier density changed easily in order of  $10^{19}$  by thermal treatment, the change by deuteron bombardment could not be detected. The number of the displaced atoms per unit volume from their regular sites by deuteron bombardment are given approximately by  $\rho(Z/M)\sigma N$ , where  $\rho$ ,  $Z$  and  $M$  are density, atomic number and mass number respectively and  $\sigma$  is the cross section of collision of the atom with deuteron and  $N$  is the number of irradiating deuterons per  $\text{cm}^2$ . In our experimental condition, if the carrier density change is proportional to the deficient number of oxygen atoms, it is anticipated that to obtain the positive results the cross section of collision must be larger than 0.1 barns. Our negative result may suggest smaller cross section of collision between oxygen atom and deuteron.

## § 6. Summary

The electrical and optical properties of tin oxide films prepared by the spraying method were studied. The experiments carried out so far show that tin oxide is a conductor with  $n$ -type carriers and the optical properties in the near infrared region is influenced strongly by the properties of free carriers. In order to unify the optical and electrical measurement, the effective mass of the carriers must be taken as  $1/5 \sim 1/7$  of the free



electron mass and the scattering index of the carriers  $p$  equal to 3. Compared with metals, tin oxide has some advantages in investigating the electric conduction mechanism and optical properties of free carriers, since the samples are transparent for wide frequency region and the specimens with the different carrier concentration can be prepared easily.

The authors wish to express their thanks to Mr. Kin'ichi Nakamura of N.H.K. for the presentation of the problem, to Mr. T. Kurachi and Prof. K. Kudo for their help in the infrared measurements, to Mr. M. Kuriyama and Prof. S. Takagi for the identification of the diffraction pattern and also to Prof. K. Takahashi for measurement of high resistance.

Furthermore, the authors wish to express their thanks to Dr. Hisao Miyazawa and Prof. Jiro Yamashita for their advices regarding several general properties of semiconductors.

### References

- 1) H. A. McMaster: Chem. Abst. **41** (1948) 3925d, US Patent 2429420.  
M. J. Zunick: Chem. Abst. **44** (1950) 11054e, US Patent 2516663.  
J. M. Mochel: Chem. Abst. **45** (1951) 1318e, US Patent 2522531.  
J. K. Davis: Chem. Abst. **46** (1952) 228a, US Patent 2564577.  
J. M. Mochel: Chem. Abst. **46** (1952) 228b, US Patent 2564707, 2564987, 2564709, 2564710, 2564705, 2564708.  
R. A. Gaiser and J. W. McAuley: Chem. Abst. **45** (1951) 10535i, US Patent 2567331.  
W. O. Lytle and A. E. Junge: Chem. Abst. **46** (1952) 1373i, US Patent 2566346.  
R. L. Gaiser: Chem. Abst. **46** (1952) 9234h, US Patent 2602032.  
M. S. Tarnopol: Chem. Abst. **46** (1952) 11616i, US Patent 2606566.
- R. F. Raymond and B. J. Dennison: Chem. Abst. **47** (1953) 7751g, US Patent 2617745.
- W. O. Lytle and A. E. Junge: Chem. Abst. **48** (1954) 971c, US Patent 2651585.
- T. K. Young and J. W. McAuley: Chem. Abst. **48** (1954) 6293e, US Patent 2667428.
- R. Gomer: Rev. Sci. Inst. **24** (1953) 993.
- 2) E. J. W. Verwey: *Semiconducting materials* (Conference at Reading) 151 (1951).  
F. A. Kroger and H. J. Vink: Physica XX (1954) 950,
- 3) R. E. Aitchison: Aust. J. App. Sci. **5** (1954) 10.
- 4) G. Bauer: Ann. d. Phys. **30** (1937) 433.
- 5) A. H. Wilson: The theory of metals 2nd ed. (1953) 232.
- 6) G. Kuwabara and K. Ishiguro: J. Phys. Soc. Japan **7** (1952) 72.
- 7) F. Abelés: J. Phys. et Rad. **11** (1950) 366.
- 8) E. Kanai: Report of Asahi Glass Co. V No. 1 (1955) 60 (in Japanese).  
A. Fischer: Z. Naturforsch. **9a** (1954) 508.
- 9) H. Y. Fan and M. Becker: *Semiconducting materials* (Conference at Reading) 145 (1951).  
E. Groschwitz and R. Wiesener: Z. Angew. Phys. **8** (1956) 391.  
J. S. Benedict and W. Shockley: Phys. Rev. **89** (1953) 1152.
- 10) K. Ishiguro and G. Kuwabara: *Methods of optical measurement, Series of Modern Physics*, Iwanami Press (1955), (in Japanese).
- 11) L. Holland and G. Siddall: Vacuum III (1953).  
A. Thelen and H. König: Naturwissenschaften **43** (1956) 297.  
F. Lappe: Z. Phys. **137** (1954) 380.
- 12) C. A. Coulson: Valence (1952) 134.  
Added references in proof.
- 13) W. G. Spitzer and H. Y. Fan: Phys. Rev. **106** (1957) 882.  
W. G. Spitzer and H. Y. Fan: Phys. Rev. **108** (1957) 268.